Gluon propagation at finite temperature

Paulo Silva, Orlando Oliveira
Center for Physics, University of Coimbra

David Dudal, Martin Roelfs
KU Leuven, campus Kortrijk

Pedro Bicudo, Nuno Cardoso
CFTP, IST, University of Lisbon

June 11, 2018

CFisUC

Outline

QCD Phase Diagram

- study of the phase diagram of QCD relevant e.g. for heavy ion experiments
- QCD has phase transition where quarks and gluons become deconfined for sufficiently high T
- Polyakov loop
  - order parameter for the confinement-deconfinement phase transition
  - $L = \langle L(\vec{x}) \rangle \propto e^{-F_q/T}$
  - Definition on the lattice:

$$L(\vec{x}) = \mathrm{Tr} \prod_{t=0}^{N_t-1} \mathcal{U}_4(\vec{x}, t)$$

  - $T < T_c$: $L = 0$ (center symmetry)
  - $T > T_c$: $L \neq 0$ (spontaneous breaking of center symmetry)

Center symmetry

- Wilson gauge action is invariant under a center transformation
- temporal links on a hyperplane $x_4 = const$ multiplied by

$$z \in Z_3 = \{e^{-i2\pi/3}, 1, e^{i2\pi/3}\}$$

- Polyakov loop $L(\vec{x}) \to zL(\vec{x})$
- $T < T_c$
  - local P_L phase equally distributed among the three sectors

$$L = \langle L(\vec{x}) \rangle \approx 0$$

- $T > T_c$
  - Z_3 sectors not equally populated: $L \neq 0$

G. Endrödi, C. Gattringer, H.-P. Schadler, arXiv:1401.7228
C. Gattringer, A. Schmidt, JHEP **01**, 051 (2011)
C. Gattringer, Phys. Lett. **B 690**, 179 (2010)

F. M. Stokes, W. Kamleh, D. B. Leinweber, arXiv:1312.0991

QCD Green's functions

- In a Quantum Field Theory, knowledge of all Green's functions allows a complete description of the theory
- In QCD, propagators of fundamental fields (e.g. quark, gluon and ghost propagators) encode information about non-perturbative phenomena
  - In particular, gluon propagator encodes information about confinement/deconfinement
- Since the gluon propagator is a gauge dependent quantity, we need to choose a gauge
  - in our works: Landau gauge

CFisUC

Gluon propagator at finite temperature

$$D^{ab}_{\mu\nu}(\hat{q}) = \delta^{ab}\left(P^T_{\mu\nu} D_T(q_4,\vec{q}) + P^L_{\mu\nu} D_L(q_4,\vec{q})\right)$$

- Two components:
  - transverse D_T
  - longitudinal D_L

$$\begin{aligned} D^{aa}_{ii}(q) &= \frac{2}{V}\left\langle \mathrm{Tr}\left[A_i(\hat{q})A^\dagger_i(\hat{q})\right]\right\rangle = \delta^{aa}\left(P^T_{ii}D^T + P^L_{ii}D^L\right) \\ D^{aa}_{44}(q) &= \frac{2}{V}\left\langle \mathrm{Tr}\left[A_4(\hat{q})A^\dagger_4(\hat{q})\right]\right\rangle = \delta^{aa}\left(P^T_{44}D^T + P^L_{44}D^L\right) \end{aligned}$$

- Finite temperature on the lattice: $L_t << L_s$

$$T = \frac{1}{aL_t}$$

CFisUC

Lattice setup finite T

Temp. (MeV)	β	L_s	L_t	a [fm]	1/a (GeV)
121	6.0000	64	16	0.1016	1.943
162	6.0000	64	12	0.1016	1.943
194	6.0000	64	10	0.1016	1.943
243	6.0000	64	8	0.1016	1.943
260	6.0347	68	8	0.09502	2.0767
265	5.8876	52	6	0.1243	1.5881
275	6.0684	72	8	0.08974	2.1989
285	5.9266	56	6	0.1154	1.7103
290	6.1009	76	8	0.08502	2.3211
305	5.9640	60	6	0.1077	1.8324
305	6.1326	80	8	0.08077	2.4432
324	6.0000	64	6	0.1016	1.943
366	6.0684	72	6	0.08974	2.1989
397	5.8876	52	4	0.1243	1.5881
428	5.9266	56	4	0.1154	1.7103
458	5.9640	60	4	0.1077	1.8324
486	6.0000	64	4	0.1016	1.943

- Simulations: use of Chroma and PFFT libraries
- keep a constant (spatial) physical volume $\sim (6.5fm)^3$
- all data renormalized at $\mu = 4GeV$

O. Oliveira, PJS, PoS(LATTICE2012)216

Acta Phys.Polon.Supp. 5 (2012) 1039

PoS(Confinement X)045

Surface plots ($q_4 = 0$)

Longitudinal component

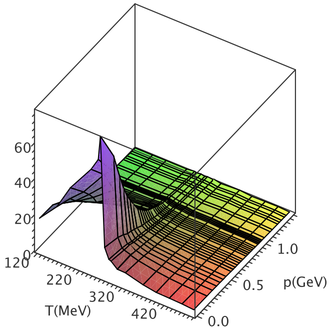

Transverse component

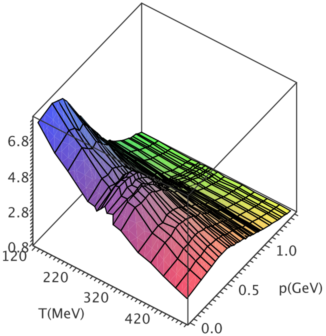

Gluon propagator @ finite T ($q_4 > 0$)

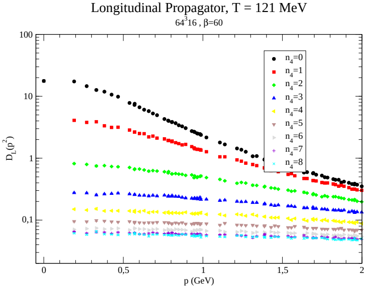

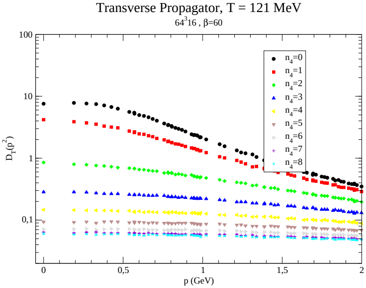

smaller D in the infrared → larger mass scales

Gluon propagator @ finite T ($q_4 > 0$)

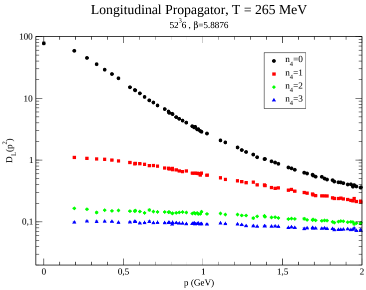

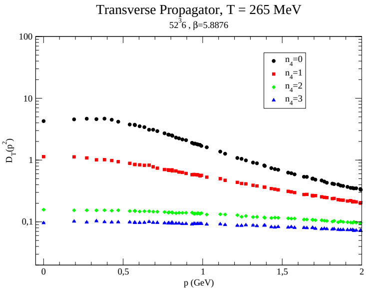

Gluon propagator @ finite T ($q_4 > 0$)

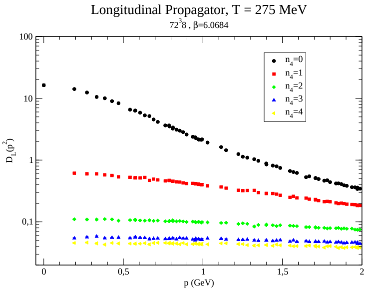

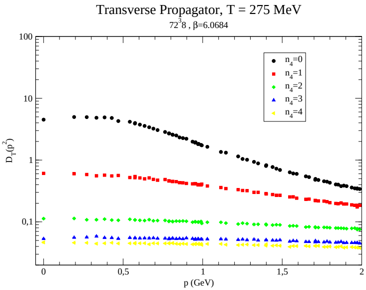

Gluon propagator @ finite T ($q_4 > 0$)

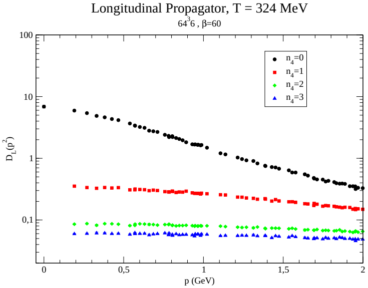

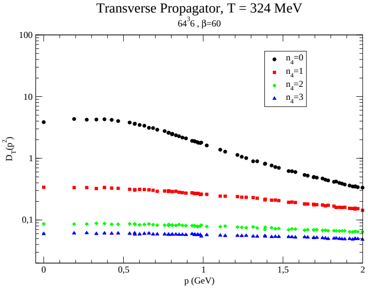

O(4) scaling

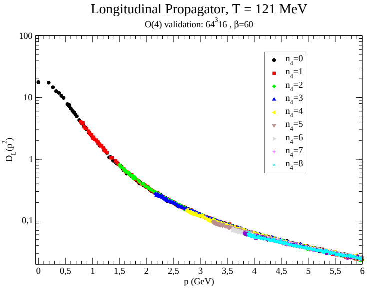

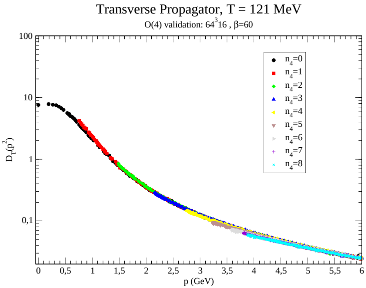

$$D(q_4, \vec{q}) = D(0, \sqrt(q_4^2 + \vec{q}^2))$$

CFisUC

O(4) scaling

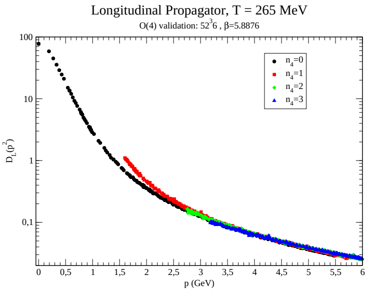

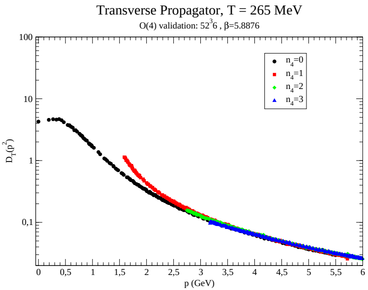

small violation for a few temperatures below T_c

O(4) scaling

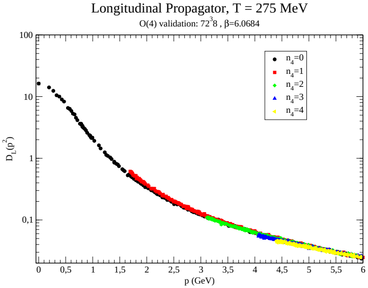
Longitudinal Propagator, T = 275 MeV
O(4) validation: 72³8 , β=6.0684
$D_L(p^2)$
p (GeV)
n4=0
n4=1
n4=2
n4=3
n4=4

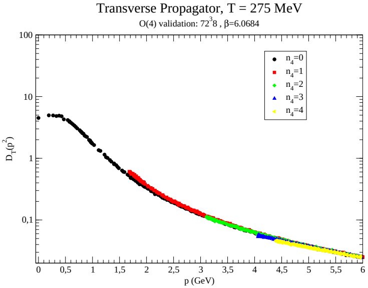
Transverse Propagator, T = 275 MeV
O(4) validation: 72³8 , β=6.0684
$D_T(p^2)$
p (GeV)
n4=0
n4=1
n4=2
n4=3
n4=4

O(4) scaling

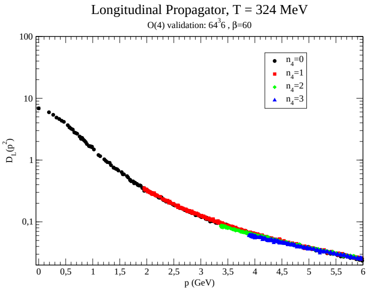
Longitudinal Propagator, T = 324 MeV
O(4) validation: $64^3 6$, β=60
$D_L(p^2)$
p (GeV)
n_4=0
n_4=1
n_4=2
n_4=3

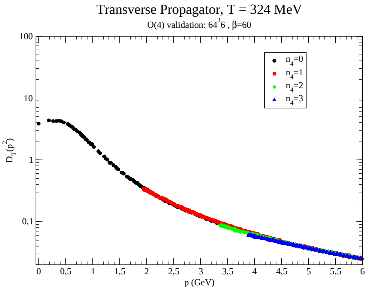
Transverse Propagator, T = 324 MeV
O(4) validation: $64^3 6$, β=60
$D_T(p^2)$
p (GeV)
n_4=0
n_4=1
n_4=2
n_4=3

Dependence on q_4

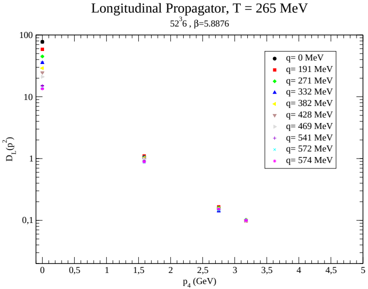

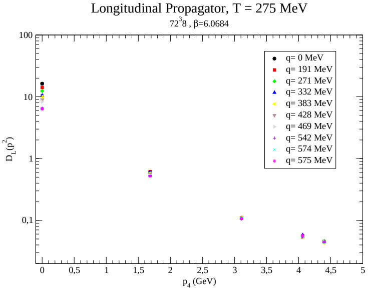

Outline

Spectral density

- Euclidean momentum-space propagator of a (scalar) physical degree of freedom

$$\mathcal{G}(p^2) \equiv \langle \mathcal{O}(p)\mathcal{O}(-p)\rangle$$

- Källén-Lehmann spectral representation

$$\mathcal{G}(p^2) = \int_0^\infty \mathrm{d}\mu \frac{\rho(\mu)}{p^2+\mu}\,, \qquad \text{with } \rho(\mu) \geq 0 \text{ for } \mu \geq 0\,.$$

- spectral density contains information on the masses of physical states described by the operator $\mathcal{O}$

$$\rho(\mu) = \sum_\ell \delta(\mu - m_\ell^2)\, |\langle 0|\mathcal{O}|\ell_0\rangle|^2\,,$$

Spectral density: motivation

- Main goal: compute the spectral density of gluons and other (un)physical degrees of freedom
  - important for e.g. DSE/BSE spectrum studies (Minkowski space)
  - spectral density is not strictly positive
  - traditional Maximum Entropy Method does not allow negative spectral densities

D. Dudal, O. Oliveira, PJS, PRD 89 (2014) 014010

Spectral density

- $\mathcal{G} = \mathcal{L}^2\hat{\rho} = \mathcal{L}\mathcal{L}^*\hat{\rho}$ where $(\mathcal{L}f)(t) \equiv \int_0^\infty ds e^{-st} f(s)$ is a Laplace transform
- inversion of Laplace transform: ill-posed problem
- Way out: Tikhonov regularization
  - ill-posed problem $y = \mathcal{K}x$
  - minimize $||\mathcal{K}x - y|| + \lambda||x||^2$
    - $\lambda > 0$ is a regularization parameter
  - x^λ is the unique solution of the normal equation

$$\mathcal{K}^*\mathcal{K}x^\lambda + \lambda x^\lambda = \mathcal{K}^* y$$

  the operator $\mathcal{K}^*\mathcal{K} + \lambda$ is strictly positive, hence invertible
- Morozov discrepancy principle: choose $\overline{\lambda}$ s.t. $||\mathcal{K}x^{\overline{\lambda}} - y^\delta|| = \delta$
  - δ: "noise of input data"
  - A unique solution $x^{\overline{\lambda},\delta}$ exists

Getting gluon spectral density

$D = \mathcal{L}^2 \rho$

- setting $D_i \equiv D(p_i^2)$; N data points
- minimization of

$$\mathcal{J}_\lambda = \sum_{i=1}^{N} \left[\int_{\mu_0}^{+\infty} \mathrm{d}\mu \frac{\rho(\mu)}{p_i^2 + \mu} - D_i \right]^2 + \lambda \int_{\mu_0}^{+\infty} \mathrm{d}\mu \; \rho^2(\mu)$$

- linear perturbation of ρ: vanishing of

$$\sum_{i=1}^{N} \underbrace{\left[\int_{\mu_0}^{+\infty} \mathrm{d}\nu \frac{\rho(\nu)}{p_i^2 + \nu} - D_i \right]}_{\equiv c_i} \frac{1}{p_i^2 + \mu} + \lambda \rho(\mu) = 0 \;\; (\mu \geq \mu_0)$$

D. Dudal, O. Oliveira, PJS, PRD **89** (2014) 014010

Getting gluon spectral density

- Källén-Lehmann inverse given by

$$\rho_\lambda(\mu) = -\frac{1}{\lambda}\sum_{i=1}^{N}\frac{c_i}{p_i^2+\mu}\theta(\mu-\mu_0)\,,$$

- linear system for coefficients c_i: $\lambda^{-1}\mathcal{M}c + c = -D$

$$\mathcal{M}_{ij} = \int_{\mu_0}^{+\infty} \mathrm{d}\nu \frac{1}{p_i^2+\nu}\frac{1}{p_j^2+\nu} = \frac{\ln\frac{p_j^2+\mu_0}{p_i^2+\mu_0}}{p_j^2-p_i^2}\,.$$

CFisUC

Getting gluon spectral density

- Reconstructed propagator:

$$D^{reconstructed}(p^2) = \int_{\mu_0}^{+\infty} \mathrm{d}\mu \frac{\rho_\lambda(\mu)}{p^2+\mu} = -\frac{1}{\lambda}\sum_{i=1}^{N} \frac{c_i \ln \frac{p^2+\mu_0}{p_i^2+\mu_0}}{p^2-p_i^2} .$$

Spectral density at finite temperature

$$\mathcal{D}(q_4,\vec{q}) = \int_0^\infty \mathrm{d}\mu \frac{\rho(\mu,\vec{q})}{q_4^2+\mu}$$

- Problem: small number of Matsubara frequencies
- How does the inversion look like when we consider just a few data points?
- Preliminary results just for $\vec{p}=(1,0,0)$

Spectral density — test T=0

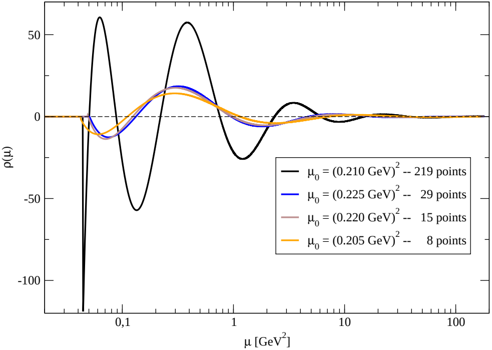

Tranverse component, T=121 MeV

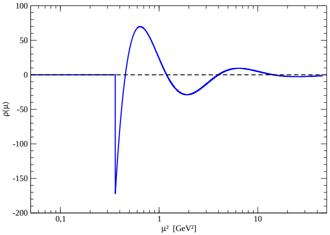

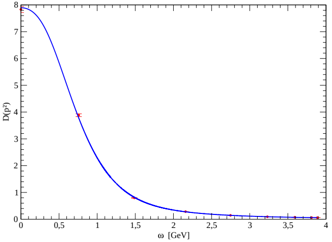

Transverse component, T=243 MeV

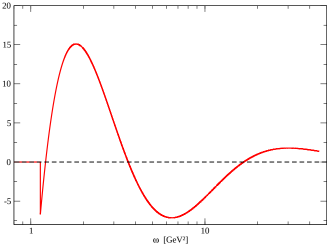

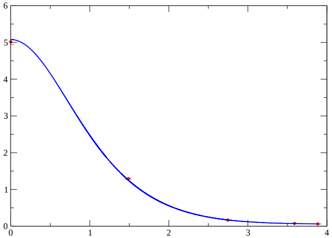

Transverse component, T=275 MeV

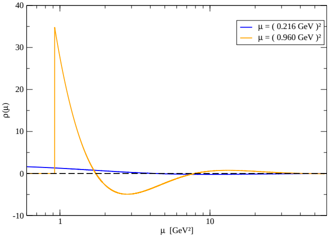

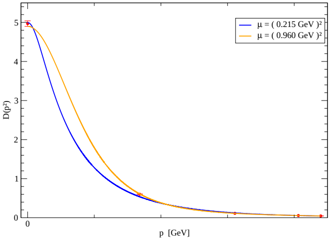

Transverse component, T=290 MeV

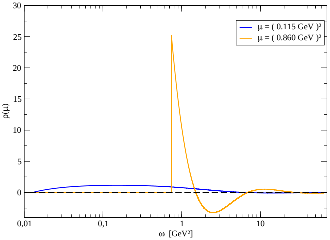

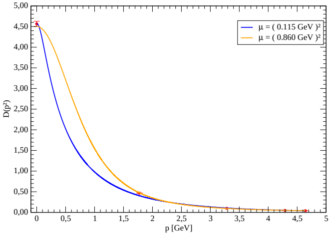

Transverse component, T=305 MeV

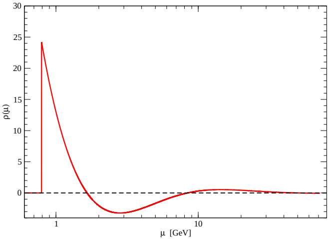

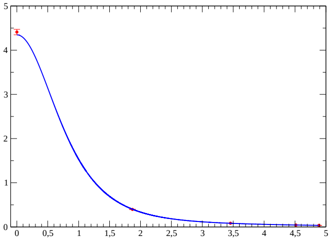

Longitudinal component, T=121 MeV

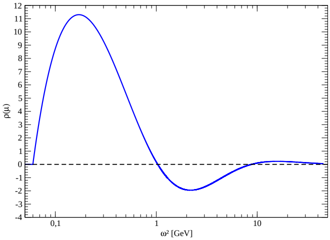

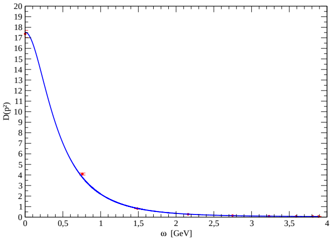

Longitudinal component, T=243 MeV

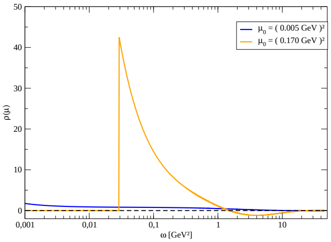

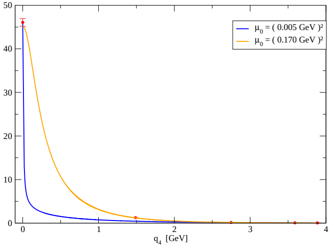

Longitudinal component, T=260 MeV

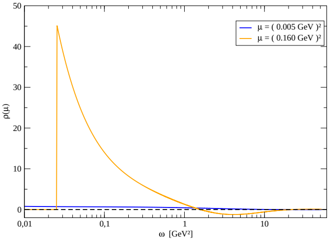

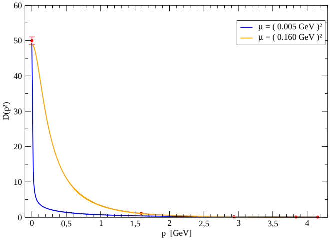

Longitudinal component, T=275 MeV

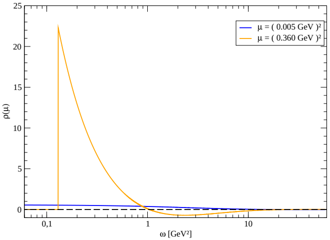

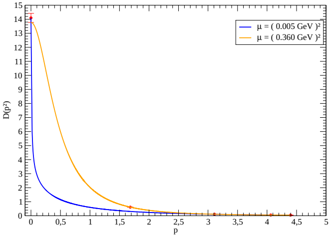

Longitudinal component, T=290 MeV

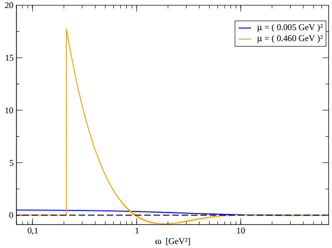

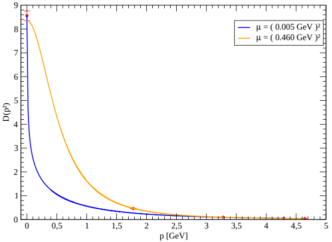

Longitudinal component, T=305 MeV

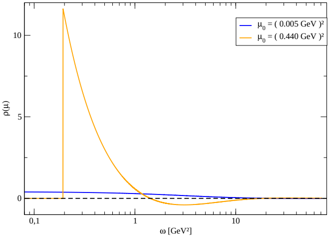

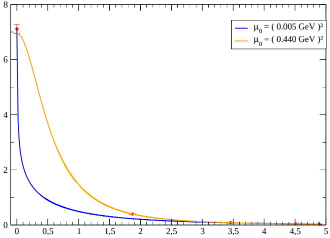

Infrared cut-offs

Longitudinal

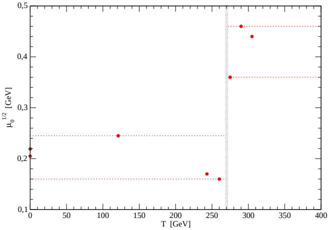

Transverse

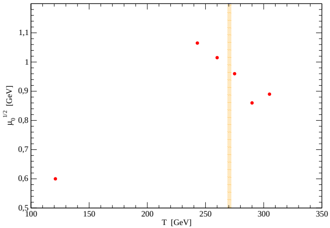

IR cut-off is sensitive to the phase transition

Outline

Why gluon mass?

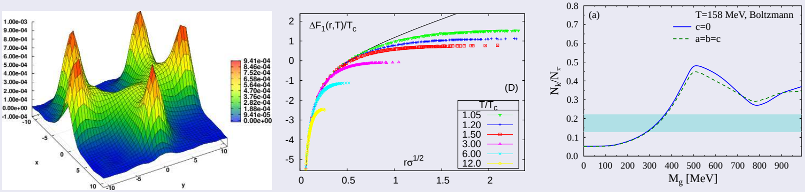

- At $T = 0$ we have colour screening and flux tubes,

J. M. Cornwall, Phys. Rev. D 26, 1453 (1982)
N. Cardoso, P. Bicudo, Phys. Rev. D 87, 034504 (2013)
N. Cardoso, M. Cardoso, P. Bicudo [arXiv:1302.3633 [hep-lat]]

- at large T Debye screening,

M. Doring, K. Hubner, O. Kaczmarek, and F. Karsch, Phys. Rev. D 75, 054504 (2007)
M. Bluhm, B. Kampfer and K. Redlich, Phys. Rev. C 84, 025201 (2011)

- at T_c a mass scale in the π and K multiplicities in heavy ions

P. Bicudo, F. Giacosa, E. Seel Phys.Rev. C86, 034907 (2012)

Gluon mass at finite T

naive M_L and M_T function of T

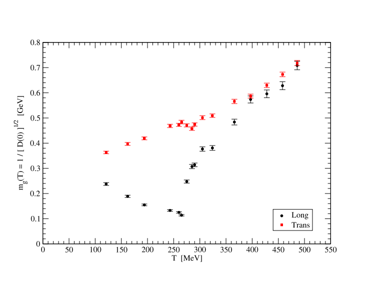

Interpretation

- The simplest ansatz for a massive propagator is,

$$D(p) = \frac{1}{p^2 + M^2}$$

$$\Rightarrow M = 1/\sqrt{D(0)}$$

PJS, O. Oliveira, P. Bicudo, N. Cardoso, Phys.Rev. D89 (2014) 074503

CFisUC

Gluon mass at finite T

- for a better IR ansatz, we fit D_i using a Yukawa fit with mass M

$$D_i(p^2) = \frac{Z}{p^2 + m^2}$$

  and look for the largest fitting range p_{max}
- this fits quite well D_L
- the Yukawa does not fit D_T

Fits of the longitudinal propagator

T	p_{max}	Z_L	M_L	$\chi^2/d.o.f.$
121	0.467	4.28(16)	0.468(13)	1.91
162	0.570	4.252(89)	0.3695(73)	1.66
194	0.330	5.84(50)	0.381(22)	0.72
243	0.330	8.07(67)	0.374(21)	0.27
260	0.271	8.73(86)	0.371(25)	0.03
265	0.332	7.34(45)	0.301(14)	1.03
275	0.635	3.294(65)	0.4386(83)	1.64
285	0.542	3.12(12)	0.548(16)	0.76
290	0.690	2.705(50)	0.5095(85)	1.40
305	0.606	2.737(80)	0.5900(32)	1.30
324	0.870	2.168(24)	0.5656(63)	1.36
366	0.716	2.242(55)	0.708(13)	1.80
397	0.896	2.058(34)	0.795(11)	1.03
428	1.112	1.927(24)	0.8220(89)	1.30
458	0.935	1.967(37)	0.905(13)	1.45
486	1.214	1.847(24)	0.9285(97)	1.55

Gluon mass at finite T

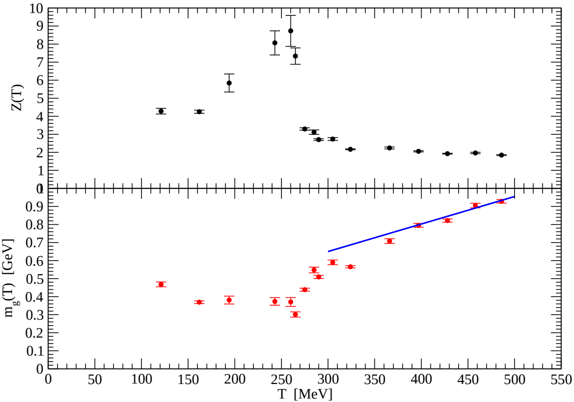

Outline

Z_3 dependence

- D_L and D_T show quite different behaviours with T
- Usually, the propagator is computed such that $\arg(P_L) < \pi/3$ (Z_3 sector 0)
- what happens in the other sectors?

PJS, O. Oliveira, PRD **93** (2016) 114509

Z_3 dependence

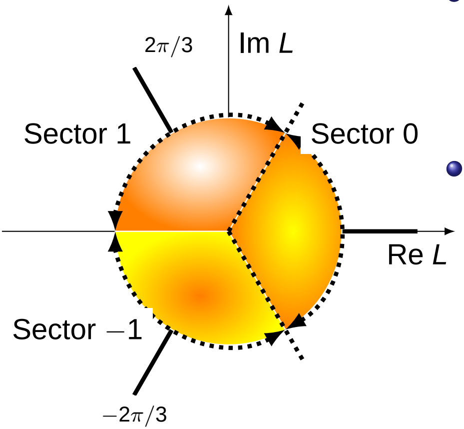

- for each configuration, 3 gauge fixings after a Z_3 transformation

$$\mathcal{U}'_4(\vec{x}, t = 0) = z\,\mathcal{U}_4(\vec{x}, t = 0)$$

- configurations classified according to $\langle L \rangle = |L| e^{i\theta}$

$$\theta = \begin{cases} -\pi < \theta \leq -\frac{\pi}{3}, & \text{Sector -1,} \\ -\frac{\pi}{3} < \theta \leq \frac{\pi}{3}, & \text{Sector 0,} \\ \frac{\pi}{3} < \theta \leq \pi, & \text{Sector 1} \end{cases}$$

Typical result at high T (324 MeV)

Longitudinal component

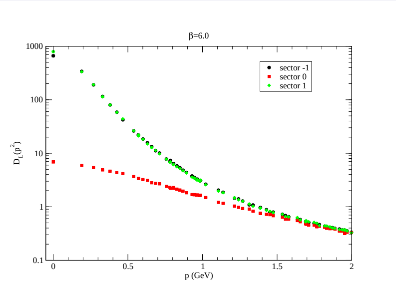

Transverse component

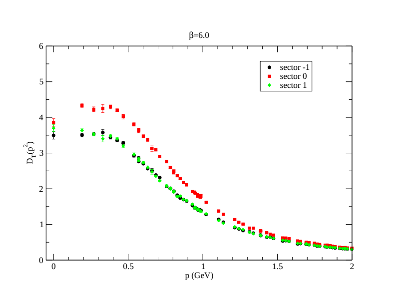

What happens near T_c ?

- spatial physical volume $\sim (6.5\text{fm})^3$
- 100 configs per ensemble

Coarse lattices $a \sim 0.12fm$

Temp. (MeV)	$L_s^3 \times L_t$	β	a (fm)	$L_s a$ (fm)
265.9	$54^3 \times 6$	5.890	0.1237	6.68
266.4	$54^3 \times 6$	5.891	0.1235	6.67
266.9	$54^3 \times 6$	5.892	0.1232	6.65
267.4	$54^3 \times 6$	5.893	0.1230	6.64
268.0	$54^3 \times 6$	5.8941	0.1227	6.63
268.5	$54^3 \times 6$	5.895	0.1225	6.62
269.0	$54^3 \times 6$	5.896	0.1223	6.60
269.5	$54^3 \times 6$	5.897	0.1220	6.59
270.0	$54^3 \times 6$	5.898	0.1218	6.58
271.0	$54^3 \times 6$	5.900	0.1213	6.55
272.1	$54^3 \times 6$	5.902	0.1209	6.53
273.1	$54^3 \times 6$	5.904	0.1204	6.50

Fine lattices $a \sim 0.09fm$

Temp. (MeV)	$L_s^3 \times L_t$	β	a (fm)	$L_s a$ (fm)
269.2	$72^3 \times 8$	6.056	0.09163	6.60
270.1	$72^3 \times 8$	6.058	0.09132	6.58
271.0	$72^3 \times 8$	6.060	0.09101	6.55
271.5	$72^3 \times 8$	6.061	0.09086	6.54
271.9	$72^3 \times 8$	6.062	0.09071	6.53
272.4	$72^3 \times 8$	6.063	0.09055	6.52
272.9	$72^3 \times 8$	6.064	0.09040	6.51
273.3	$72^3 \times 8$	6.065	0.09025	6.50
273.8	$72^3 \times 8$	6.066	0.09010	6.49

How-to

- Conical cut for momenta above 1GeV; all data below 1GeV

- Renormalization:

$$D_{L,T}(\mu^2) = Z_R D^{Lat}_{L,T}(\mu^2) = 1/\mu^2$$

- Renormalization scale: $\mu = 4$ GeV
- D_L and D_T renormalized independently
  - within each $Z(3)$ sector, $Z_R^{(L)}$ and $Z_R^{(T)}$ agree within errors
- each Z_3 sector is renormalized independently
  - Z_R do not differ between the different $Z(3)$ sectors

Coarse lattices, below T_c

Longitudinal component

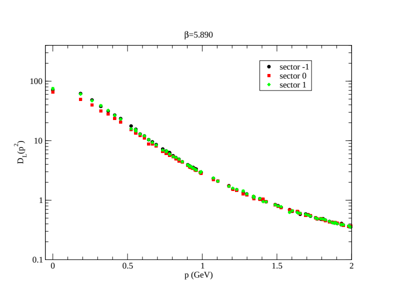

Transverse component

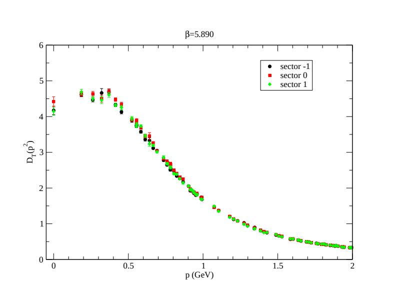

Fine lattices, below T_c

Longitudinal component

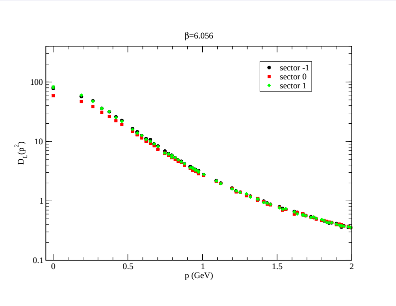

Transverse component

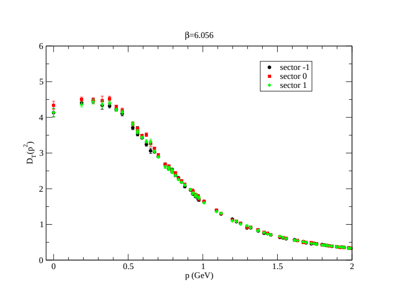

Coarse lattices, above T_c

Longitudinal component

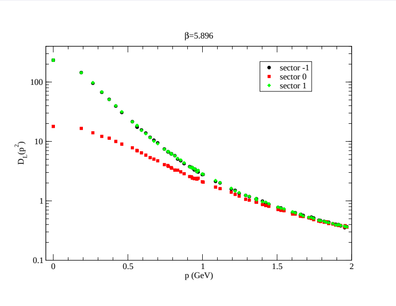

Transverse component

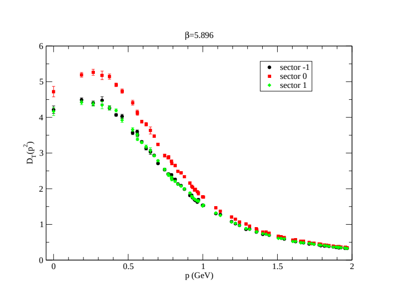

Fine lattices, above T_c

Longitudinal component

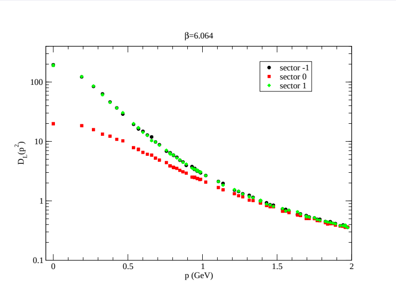

Transverse component

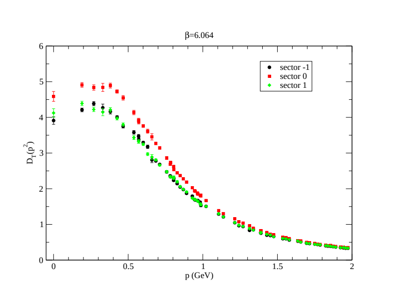

Polyakov loop history

Modulus

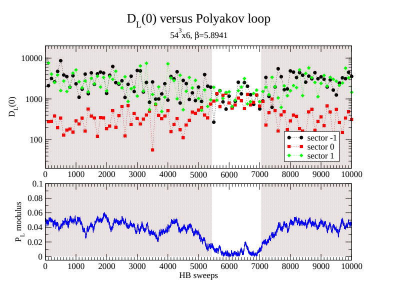

Phase

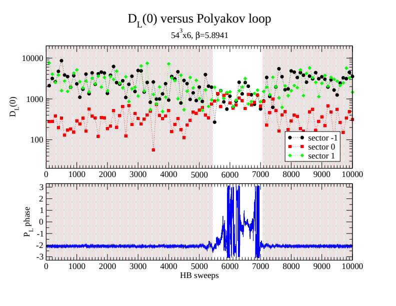

Polyakov loop history

Modulus

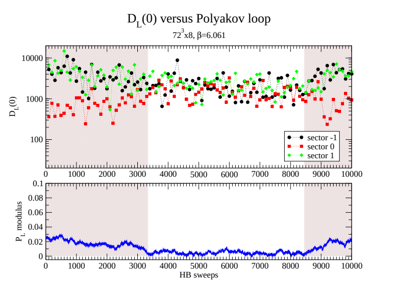

Phase

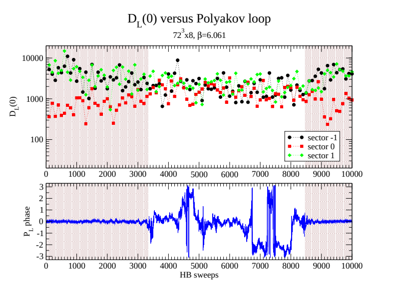

Removing configurations in wrong phase

Coarse lattices

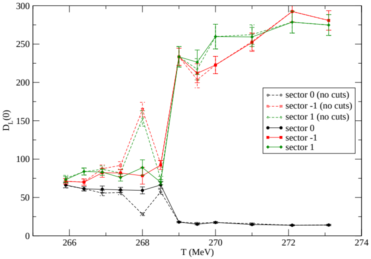

Fine lattices

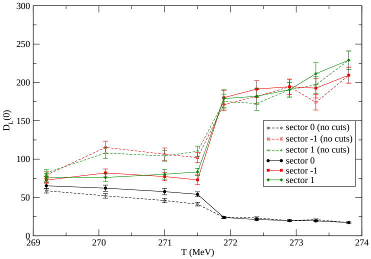

Conclusions and Outlook

- Extensive study of the gluon propagator at finite temperature
  - spectral densities
  - Mass scales
  - Z_3 dependence
- Outlook:
  - Spectral density computation ongoing
  - understand physics of different Z_3 sectors
  - lattice simulations with dynamical quarks

PJS supported by FCT grant SFRH/BPD/109971/2015.